Supporting Information

Lee et al. 10.1073/pnas.0811231106

SI Text

Solubilization of the Partially Denatured Insulin β-Chain by Complex Formation with AtTDX. Various concentrations of AtTDX were incubated with 30 μM bovine insulin and 0.5 mM DTT in 50 mM Hepes-KOH (pH 8.0) buffer. The incubation mixture was centrifuged at 25,000 × *g* at 4°C for 20 min. The soluble supernatants were separated on nonreducing SDS/PAGE gels, and subjected to silver staining.

Preparation of Truncated AtTDX Mutant Proteins for the Oligomeric Status/Function Analysis. To identify the domains responsible for AtTDX's multiple functions, a number of truncated DNA constructs were prepared by using PCR and expressed in *E. coli*. To analyze the role of Cys residues in the AtTDX protein, we replaced both Cys residues of AtTDX in the Trx motif with Ser (C304S, C307S, and a double mutant C304/307S). Although most of the AtTDX mutant proteins were highly expressed and homogeneously purified from *E. coli* (Fig. S6*B*), the truncated proteins containing amino acids 1–217, 218–380, and 112–380 were pelleted as inclusion bodies and were not included in the analyses.

Chlorophyll Content and Fluorescence Measurements. Thermotolerance of the WT *Arabidopsis* and representative T_3 lines of transgenic *Arabidopsis* plants overexpressing AtTDX (OE) and the AtTDX C304/307S mutant (C304/307S), or suppressing endogenous AtTDX protein (Sup) were analyzed by measuring the chlorophyll content and chlorophyll fluorescence. For the experiment, 4-week-old *Arabidopsis* seedlings were heat-treated at 38 °C for 5 days, transferred to their optimal growing conditions (22 °C), and then grown for an additional 5 days (recovery period), as outlined in Fig. 5*C Upper*. During the recovery period, changes in the chlorophyll quantity and chlorophyll fluorescence were examined in leaves. Chlorophyll was extracted by using 80% (vol/vol) acetone and then measured as described (1, 2). The chlorophyll fluorescence (quantum yield of PSII, Fv/Fm) was measured with a portable fluorometer (Handy PEA; Hansatech). The leaves were dark-adapted for 10 min before the measurement as described (3). At least 3 leaves from each plant line were analyzed, and the Fv/Fm ratio was estimated as described (4).

1. Arnon DI (1949) Copper enzymes in isolated chloroplasts. Polyphenoloxidase in *Beta Vulgaris*. *Plant Physiol* 24:1–15.
2. Porra RJ, Thompson WA, Kriedemann PE (1989) Determination of accurate extinction coefficients and simultaneous equations for assaying chlorophyll a and b extracted with four different solvents: Verification of the concentration of chlorophyll standards by atomic absorption spectroscopy. *Biochem Biophys Acta* 975:384–394.
3. Shahbazi M, Gilbert M, Labouré AM, Kuntz M (2007) Dual role of the plastid terminal oxidase in tomato. *Plant Physiol* 145:691–702.
4. Kang D-J, et al. (2005) Jasmonic acid differentially affects growth, ion uptake, and abscisic acid concentration in salt-tolerant and salt-sensitive rice cultivars. *J Agron Crop Sci* 191:273–282.

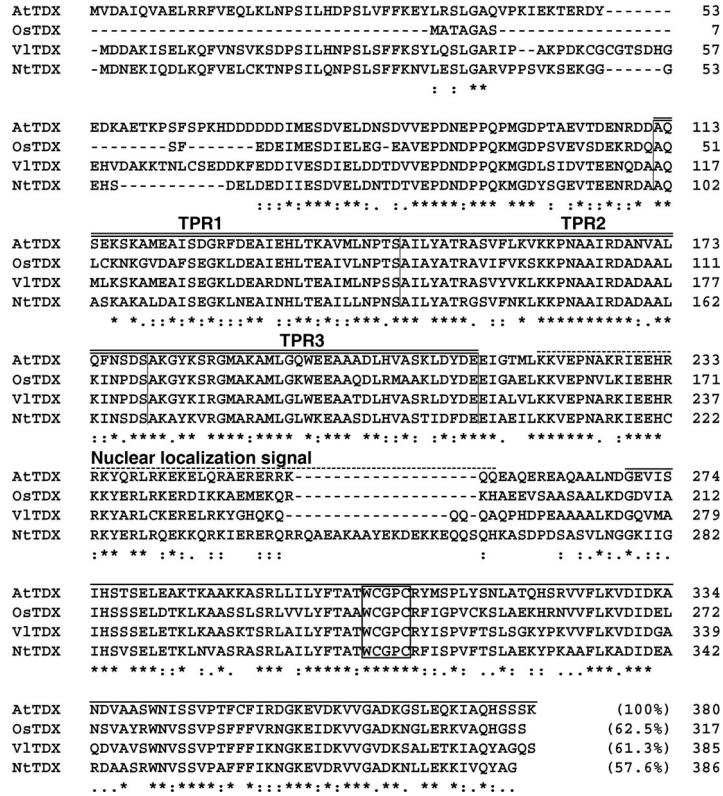

Fig. S1. Alignment of the amino acid sequence of AtTDX with other TDX proteins from plant sources. The 3 TPR domains are marked by double lines. The Trx domain is indicated by a single horizontal line, and its active site is boxed. The putative nuclear localization signal (NLS) is indicated by a dotted line. Numbers indicate protein length in amino acids. *, :, and . indicate fully-, strongly-, and weakly-conserved residues, respectively. Dashes within the sequences represent gaps introduced to optimize alignment. The GenBank accession numbers are as follows: *Arabidopsis thaliana* TDX (AtTDX: At3g17880), *Oryza sativa* TDX (OsTDX: AK063980), *Nicotiana tabacum* TDX (NtTDX: AY064253), and *Vitis labrusca* TDX (VlTDX: AY036906). Multiple alignments were analyzed by ClustalW.

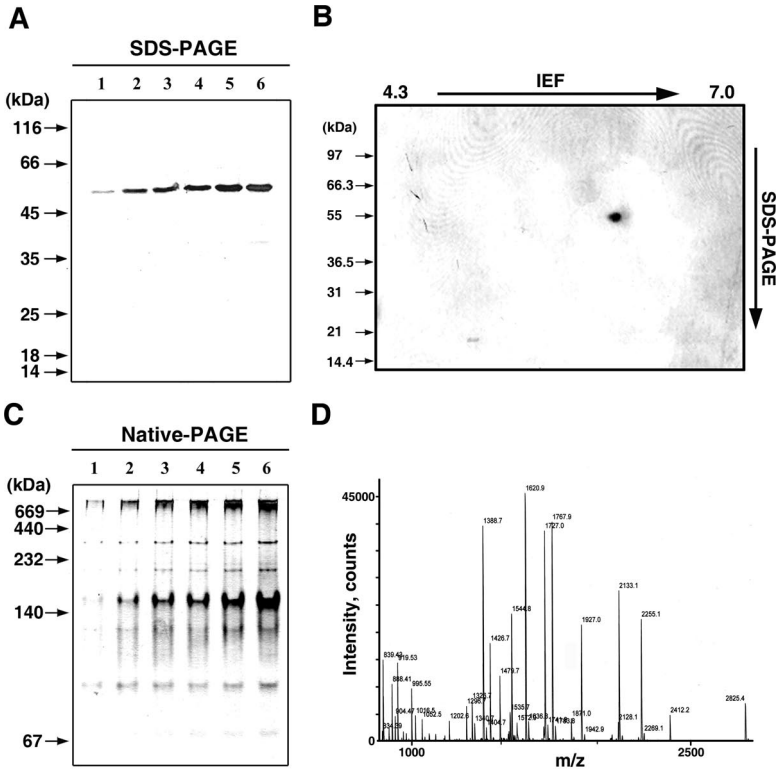

E

[–] **Detailed Results**

Acc. #: 30684711 **Species:** ARABIDOPSIS THALIANA **Name:** ATTDX (TETRATICOPEPTIDE DOMAIN-CONTAINING THIOREDOXIN); thiol-disulfide exchange intermediate

Index: 1110946 **MW:** 42847 Da **pI:** 5.5

m/z Submitted	MH+ Matched	Intensity	Delta ppm	Modifications	Start	End	Missed Cleavages	Sequence
888.4130	888.4170	100.0	-4.49		255	261	0	(K)QQEAQER(E)
919.5320	919.5360	100.0	-4.33		12	18	1	(R)RFVEQLK(L)
1016.5210	1016.5119	100.0	8.91		254	261	1	(R)KQQEAQER(E)
1202.6070	1202.6052	100.0	1.51		128	137	0	(R)FDEAIEHLTK(A)
1426.6700	1426.6770	100.0	-4.92		209	220	0	(K)LDYDEEIGTMLK(K)
1479.7060	1479.7074	100.0	-0.955		168	181	0	(R)DANVALQFNSDSAK(G)
1620.9080	1620.8778	100.0	18.6		138	152	0	(K)AVMLNPTSAILYATR(A)
1726.9780	1726.9527	100.0	14.7		19	33	0	(K)LNPSILHDPSLVFFK(E)
1741.8160	1741.8279	100.0	-6.84		52	66	1	(R)DYEDKAETKPSFSPK(H)
1767.8770	1767.8483	100.0	16.2		309	323	0	(R)YMSPLYSNLATQHSR(V)
1870.9520	1870.9343	100.0	9.48		294	308	0	(R)LLILYFTATWCGPCR(Y)
1926.9640	1926.9378	100.0	13.6		191	208	0	(K)AMLGQWEEAAADLHVASK(L)
2133.0690	2133.0281	100.0	19.2		119	137	1	(K)AMEAISDGRFDEAIEHLTK(A)
2412.2200	2412.1889	100.0	12.9		262	284	0	(R)EAQAALNDGEVISIHSTSELEAK(T)
2825.4340	2825.3927	100.0	14.6		329	353	1	(K)VDIDKANDVAASWNISSVPTFCFIR(D)

Fig. S2. Homogeneity analysis of purified AtTDX by electrophoresis and MALDI-TOF mass spectrometry. (*A*–*C*) Various concentrations of AtTDX were separated on 12% reducing SDS/PAGE (*A*), 2D PAGE (*B*), and 10% native PAGE (*C*) gels and stained with silver staining. (*D* and *E*) The single protein spot obtained from separating 2 μg of AtTDX by 2D PAGE (*B*) was subjected to MALDI-TOF analysis (*D*), which identified the protein as being AtTDX (*E*). The following amounts of AtTDX protein were loaded onto SDS/PAGE and native PAGE gels: 0.2 μg (lanes 1), 0.4 μg (lanes 2), 0.6 μg (lanes 3), 0.8 μg (lanes 4), 1.0 μg (lanes 5), and 2 μg (lanes 6). IEF, isoelectric focusing.

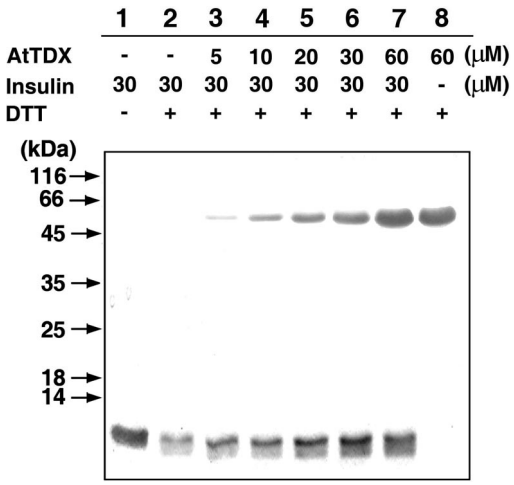

Fig. S3. Solubilization of the reduced and partially-denatured insulin β-chain by complex formation with AtTDX. Various concentrations of AtTDX were incubated with 30 μM insulin in the absence (−) or presence (+) of 0.5 mM DTT at room temperature for 25 min. After centrifuging the reaction mixture (25,000 × *g*, 20 min), the soluble supernatant proteins were subjected to 15% reducing SDS/PAGE, followed by silver staining, which showed that the solubility of the DTT-mediated reduced and partially-denatured β-chain of insulin is proportionally increased by increasing the concentration of AtTDX in the reaction mixture.

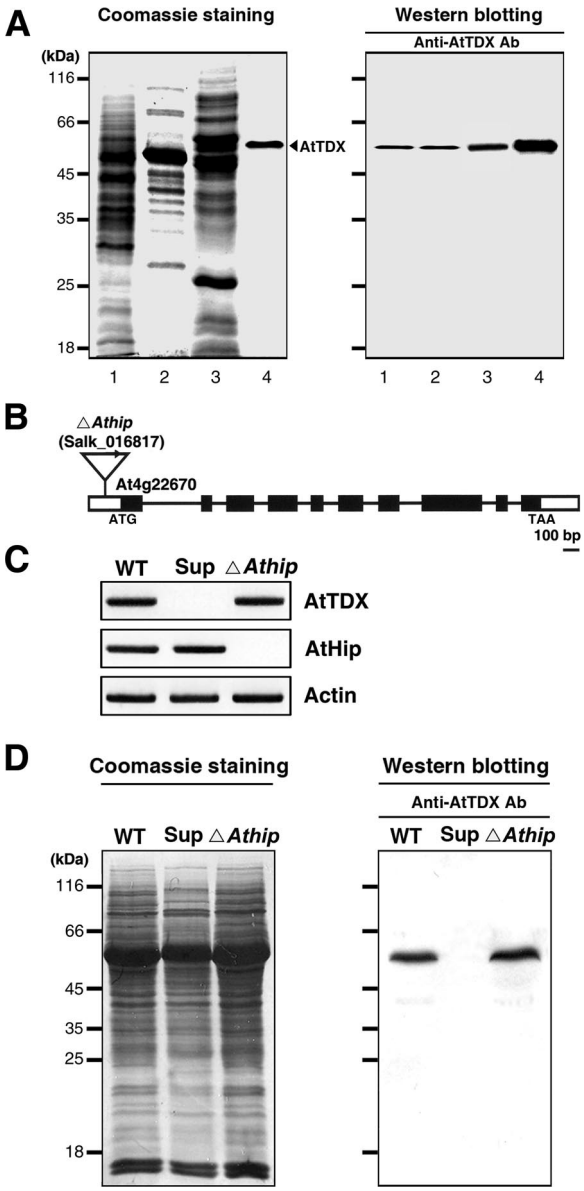

Fig. S4. Immuno-specificity of the anti-AtTDX antibody. (*A*) Soluble proteins (50 μg) extracted from *Arabidopsis* seedlings grown for 4 weeks (lane 1), *Arabidopsis* suspension cells (lane 2), *E. coli* cells overexpressing AtTDX (lane 3), and purified recombinant AtTDX (1 μg) (lane 4) were separated on a 12% reducing SDS/PAGE gel and stained with Coomassie brilliant blue (Coomassie staining). Proteins resolved by SDS/PAGE were transferred onto a nitrocellulose membrane for Western blot analysis and probed with a 1:20,000 (vol/vol) dilution of a polyclonal antibody raised against AtTDX by using the alkaline phosphatase assay, which resulted in a specific immune-reaction of the antibody with AtTDX. (*B–D*) Antibody specificity of AtTDX was analyzed by using WT *Arabidopsis*, a transgenic *Arabidopsis* line suppressing AtTDX (Sup), and a T-DNA insertion Δ*Athip* knockout line of *Arabidopsis* (Salk line 016817). (*B*) Position of the T-DNA insertion site in AtHIP genomic DNA. The AtHIP genomic cDNA includes 10 exons (black boxes), 9 introns (bold lines between black boxes) and untranslated regions (UTR: white boxes). ATG, initiation codon; TAA, stop codon. (*C*) Expression levels of the mRNAs encoding AtTDX and AtHIP were gauged by RT-PCR in WT *Arabidopsis*, transgenic *Arabidopsis* suppressing AtTDX (Sup), and the *Arabidopsis* T-DNA insertion knockout mutant Δ*Athip*. (*D*) After extracting the cytosolic fractions from the *Arabidopsis* plants, they were separated on 12% SDS/PAGE gels and subjected to either Coomassie blue staining (*Left*) or Western blot analysis (*Right*) with an anti-AtTDX antibody. The anti-AtTDX antibody immuno-reacted specifically with AtTDX.

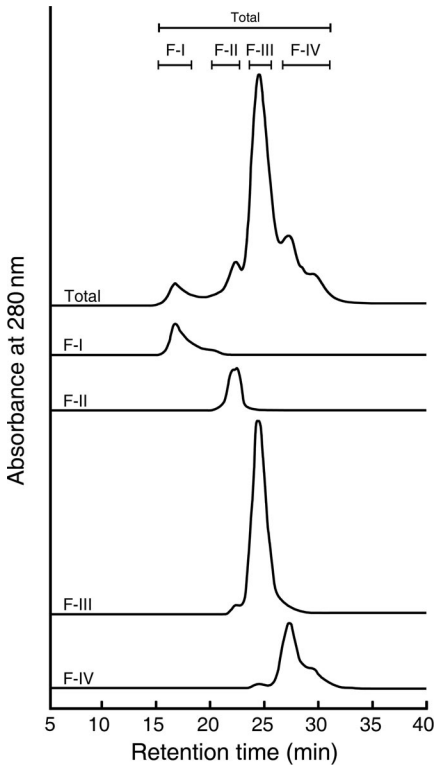

Fig. S5. Rechromatography of the four AtTDX protein fractions (F-I–F-IV) separated by SEC. The SEC-separated protein fractions (F-I–F-IV) of AtTDX were concentrated and rechromatographed by SEC under the same conditions as in Fig. 2*A*. The functional activity of each fraction was characterized.

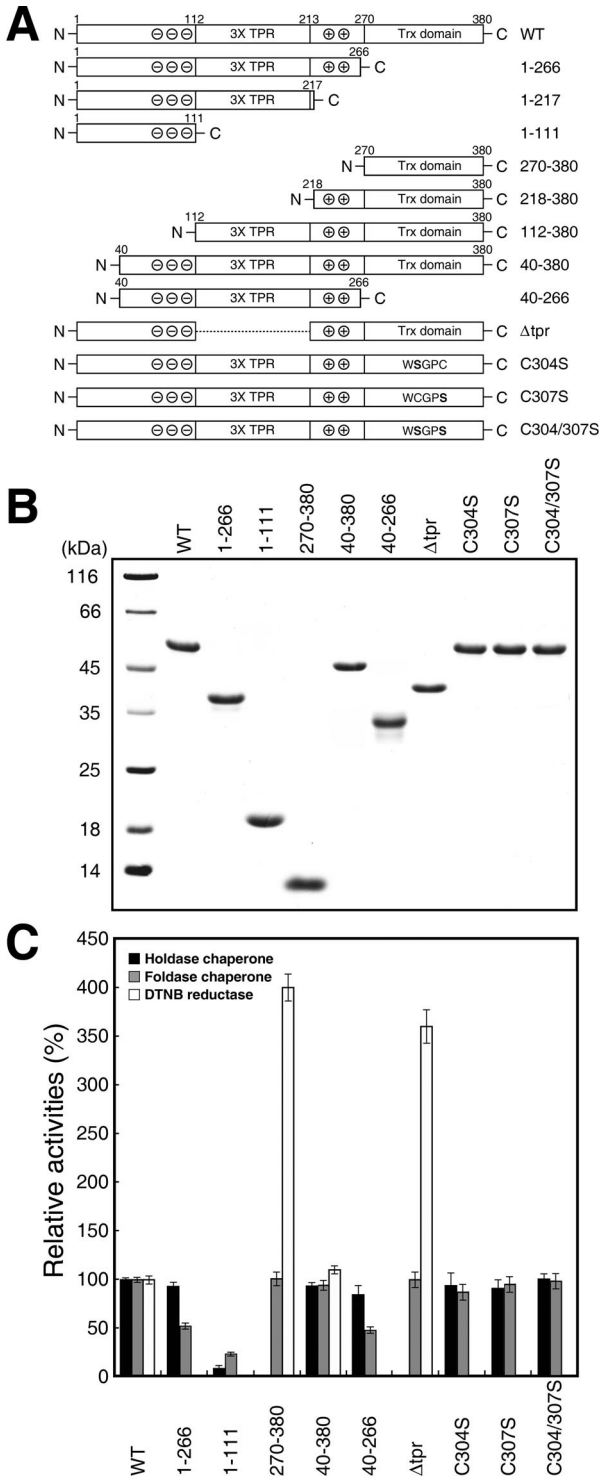

Fig. S6. Functional analysis of the various forms of truncated AtTDX. (*A*) A schematic representation of the truncated forms of recombinant AtTDX. (*B*) AtTDX deletion constructs were expressed in *E. coli* and purified by affinity chromatography. C304S, C307S, and C304/307S represent point substitutions of the Cys residues with Ser. Purified proteins of AtTDX were separated on a 12% SDS/PAGE gel and stained with Coomassie brilliant blue. First lane, molecular marker. (*C*) DTNB-reductase activity with the use of NADPH/Trx reductase as reductant (white bars), foldase chaperone activity (gray bars), and holdase chaperone activity (black bars) of various deletion mutants were compared with those of native AtTDX (WT), whose activities were set to 100%.

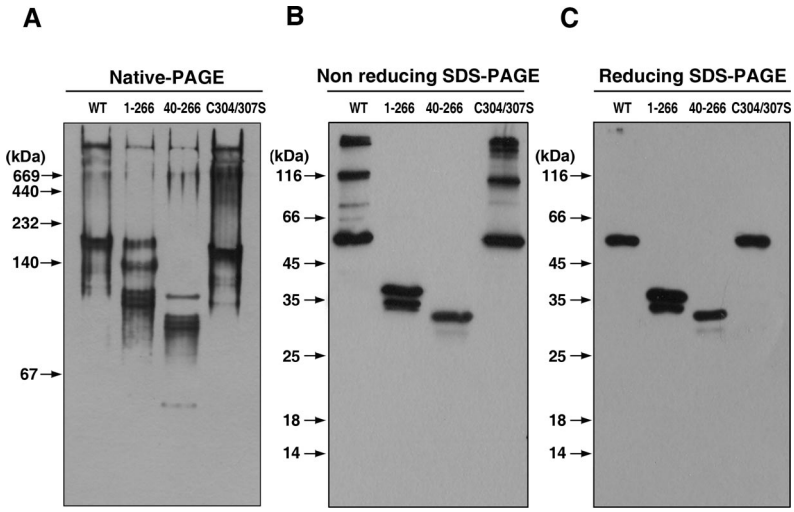

Fig. S7. Oligomerization status of native AtTDX (WT), truncated forms of AtTDX (residues 1–266 and 40–266), and Cys mutant AtTDX (C304/307S) presented in Fig. S6 analyzed by Western blotting. Purified proteins of native AtTDX (WT), various forms of truncated mutant AtTDX (residues 1–266 and 40–266), and Cys mutant AtTDX (C304/307S) were separated on 10% native-PAGE (*A*), 12% nonreducing SDS/PAGE (*B*), and reducing SDS/PAGE (*C*) gels and subjected to Western blot analysis with an anti-AtTDX antibody. The oligomerization status of the proteins was compared under the various PAGE conditions.

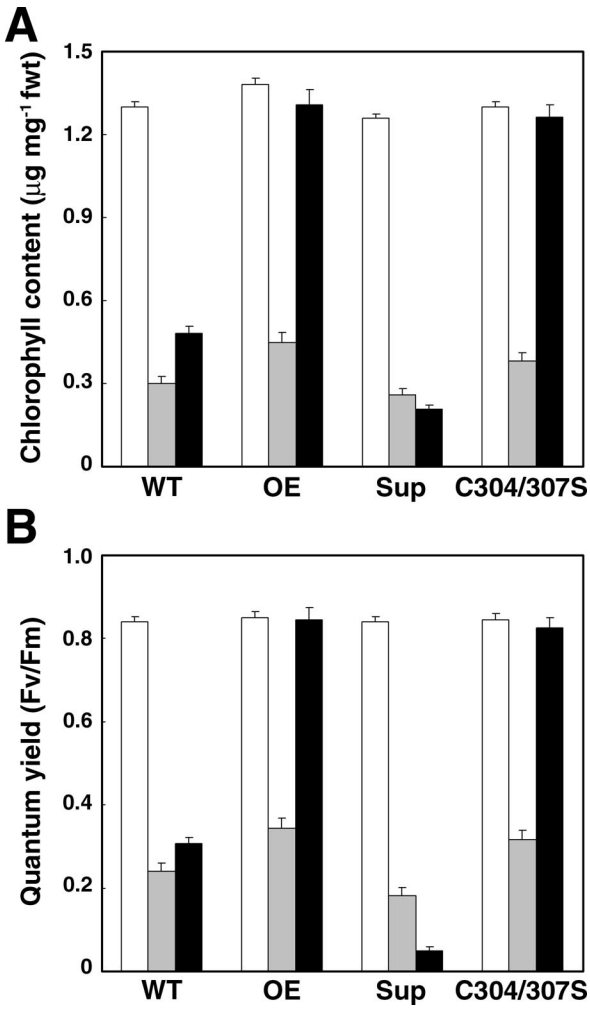

Fig. S8. Photosynthetic parameters of transgenic *Arabidopsis* plants during the recovery period from heat shock. Four-week-old T_3 homozygous lines of *Arabidopsis* grown at 22°C, including the WT, an AtTDX overexpression line (OE), an AtTDX suppression line (Sup), and a Cys-mutant-AtTDX overexpression line (C304/307S), were heat-stressed at 38 °C for 5 days and then restored to their optimal growing conditions (22 °C), as outlined in Fig. 5*C Upper*. During the heat shock and recovery periods, changes of total chlorophyll content (*A*) and steady-state quantum yield (*B*) were measured. The photosynthetic parameters of *Arabidopsis* plants grown at 22 °C (white bar; indicated by white box in Fig. 5*C*) were compared with those of plants heat-stressed at 38 °C for 5 days (gray bar; indicated by white box in Fig. 5*C*), and plants were allowed to recover from heat shock for 5 days at optimum growing conditions (22 °C) (black bar; indicated by white box in Fig. 5*C*).